

Systematics of 2^+ states in C isotopes from the *ab initio* no-core shell model

C. Forssén,^{1,*} R. Roth,² and P. Navrátil³

¹*Fundamental Physics, Chalmers University of Technology, 412 96 Göteborg, Sweden*

²*Institut für Kernphysik, Technische Universität Darmstadt, 64289 Darmstadt, Germany*

³*TRIUMF, 4004 Wesbrook Mall, Vancouver,*

British Columbia, V6T 2A3 Canada[†]

Lawrence Livermore National Laboratory,

P.O. Box 808, L-414, Livermore, CA 94551, USA

(Dated: June 3, 2019)

Abstract

We study low-lying states of even-even carbon isotopes in the range $A = 10 - 20$ within the large-scale *ab initio* no-core shell model (NCSM). Using several accurate nucleon-nucleon (NN) as well as NN plus three-nucleon (NNN) interactions, we calculate excitation energies of the lowest 2^+ state, the electromagnetic $B(E2; 2_1^+ \rightarrow 0_1^+)$ transition rates, the 2_1^+ quadrupole moments as well as selected electromagnetic transitions among other states. Recent experimental campaigns to measure 2^+ -state lifetimes indicate an interesting evolution of nuclear structure that is a challenge to reproduce theoretically from first principles. Our calculations do not include any effective charges or other fitting parameters. Overall, we find a good agreement with the experimentally observed trends, although our calculated $B(E2; 2_1^+ \rightarrow 0_1^+)$ value for ^{16}C is lower compared to the most recent measurements. Relative transition strengths from higher excited states are investigated and the influence of NNN forces is discussed. In particular for ^{16}C we find a remarkable sensitivity of the transition rates from higher excited states to the details of the nuclear interactions.

PACS numbers: 21.60.De, 21.10.Tg, 21.10.Ky, 21.30.Fe, 27.20.+n, 27.30.+t

[†] Present address.

*christian.forssen@chalmers.se

I. INTRODUCTION

Electric quadrupole (E2) matrix elements are important quantities in probing nuclear structure. In particular, they are very sensitive to nuclear deformation, the decoupling of proton and neutron degrees of freedom, and they are often affected by small components of the nuclear wave function. In this paper we study systematically the observables that are obtained from diagonal and non-diagonal E2 matrix elements in the range of even carbon isotopes, from ^{10}C to the very neutron rich ^{20}C . Quadrupole moments, corresponding to diagonal E2 matrix elements, are inherently difficult to measure for excited 2^+ states. Off-diagonal matrix elements, however, have recently been studied for several heavy carbon isotopes using lifetime measurements [1–5]. In this way, the reduced transition probability, $B(E2; 2_1^+ \rightarrow 0_1^+)$, can be extracted since it's inversely proportional to the lifetime of the 2^+ state. As a result of these experimental studies several different claims have been made on the nuclear structure in this chain of isotopes. Initial excitement was triggered by the observation of a strongly quenched E2 transition in ^{16}C [1]. Based on the liquid-drop model, which predicts the $B(E2)$ to be inversely proportional to the 2^+ excitation energy, Imai *et al.* [1] claimed an anomalous reduction of the E2 strength when comparing 2^+ lifetimes for ^{14}C ($E_{2^+} = 7.01$ MeV) and ^{16}C ($E_{2^+} = 1.77$ MeV). The $^{16}\text{C}(2^+)$ lifetime was remeasured by Wiedeking *et al.* [2] providing a much shorter value, thus indicating a larger $B(E2)$ strength. Their results were analyzed in terms of shell model calculations. Adjusting the effective neutron charge to reproduce their measured lifetimes they made the claim that the results for ^{16}C are “normal” to this region. Lifetime measurements of $^{16,18}\text{C}$ were reported by Ong *et al.* [3]. The presented results for ^{16}C came from a reanalysis of the original data [1], now giving a larger but still quenched $B(E2)$ strength, while the new ^{18}C data indicated the persistence of the quenching of E2 strengths in heavy carbon isotopes. Possible explanations were put forward in terms of the decoupling of protons and neutrons resulting in very low values for the neutron effective charges and/or the appearance of a new proton magic number $Z = 6$ in this region. Some of these statements were backed up by new shell model calculations by Fujii *et al.* [6] reproducing the $^{16,18}\text{C}$ results employing exceptionally small effective charges.

These developments provide a strong motivation to perform *ab initio* calculations, without fitting parameters, to study the evolving nuclear structure in the carbon chain of (even)

isotopes with particular focus on 2^+ states and quadrupole moments. We have, therefore, carried out large-scale *ab initio* no-core shell model (NCSM) [7] calculations for low-lying states of the even-even carbon isotopes with $A = 10 - 20$. These calculations are performed starting from realistic Hamiltonians without adjustable parameters. In particular, since our many-body scheme does not involve an inert-core approximation we will use bare charges when evaluating electromagnetic observables. Particular efforts will be made to quantify the uncertainties of the observables.

A. Theoretical formalism

The NCSM method has been described in great detail in several papers, see e.g., Ref. [8]. Here, we just outline the approach as it is applied in the present study. We start from the intrinsic Hamiltonian for the A -nucleon system $H_A = \mathcal{T}_{\text{rel}} + \mathcal{V}$, where \mathcal{T}_{rel} is the relative kinetic energy and \mathcal{V} is the sum of nuclear and Coulomb interactions. The potential term will always contain two-body operators, but we can also include three-body terms originating from an initial NNN force or induced by a unitary transformation of the Hamiltonian. This transformation is employed to soften the Hamiltonian for the description of many-body, low-energy observables and will be described below.

In this work we have used several different nuclear Hamiltonians: the pure NN interactions CD-Bonn 2000 [9] (CDB2k), based on one-boson exchange theory, and INOY [10] that introduces a nonlocality to include some effects of three-nucleon forces and is fitted also to three-nucleon observables. In addition we have used the most recent chiral NN plus NNN interaction, i.e. the $N^3\text{LO}$ NN interaction of Ref. [11] and a local chiral $N^2\text{LO}$ NNN potential with low-energy constants determined entirely in the three-nucleon system [12]. All three Hamiltonians reproduce NN phase shifts with very high precision.

We solve the many-body problem in a large but finite harmonic-oscillator (HO) basis truncated by a maximal total HO energy of the A -nucleon system. The many-body model space is usually characterized by the cutoff-parameter N_{max} , giving the maximum number of HO excitations above the unperturbed A -nucleon ground state. The diagonalization of the Hamiltonian in this many-body basis is a highly non-trivial problem because of the very large dimensions that we encounter. To solve this problem, we have used a specialized version of the shell model code ANTOINE [13], adapted to the NCSM [14]. For the runs involving

explicit NNN interactions we used the NSUITE package [15, 16], which is in addition capable of performing the importance-truncated NCSM calculations described below, and also the code NCSD [17].

Due to the strong short-range correlations generated by the NN potentials, we must calculate an effective interaction to speed up the convergence. We employ two different similarity transformations to construct the effective interactions: For CDB2k and INOY as initial NN interactions we derive two-body effective interactions appropriate to the low-energy basis truncation by a unitary transformation in the two-nucleon HO basis (Lee-Suzuki effective interaction [7, 18]). For the chiral $NN + NNN$ Hamiltonian we employ the similarity renormalization group (SRG) with the initial and induced three-body terms included consistently [16, 19].

Our results exhibit dependence on N_{\max} and the HO frequency Ω that should disappear once a complete convergence is reached. This implies that N_{\max} -sequences obtained at different HO frequencies should all converge to the same result. This feature can be utilized to perform a constrained fit to multiple sequences [20, 21]. To this end, we use as large an N_{\max} basis as feasible for a wide range of HO frequencies, and extrapolate calculated observables to infinite space. Results obtained for a range of frequencies were used in the fits. We found that the convergence with increasing N_{\max} for energy observables can be well fitted by: $x = x_{\infty} + c_0 \exp(-c_1 N_{\max})/N_{\max}$, and for EM observables by $x = x_{\infty} + c_0/N_{\max} + c_1/N_{\max}^2$. The parameters c_0 and c_1 are allowed to vary for each N_{\max} -sequence, while the parameter x_{∞} is common to all N_{\max} -sequences and gives the extrapolated result at $N_{\max} \rightarrow \infty$. An error estimate is made based on repeating the constrained fit keeping either the three highest or the three lowest frequencies in the selected range.

The current limit on the full- N_{\max} -space calculations with a two-body Hamiltonian is, e.g., $N_{\max} = 6$ for ^{18}C with a dimension of 1.4×10^9 . To reach still larger N_{\max} we employ the importance-truncated (IT) NCSM scheme [15, 22]. It makes use of the fact that many of the basis states are irrelevant for the description of a set of low-lying states. Based on many-body perturbation theory, one can define a measure for the importance of individual basis states and discard states with an importance measure below a threshold value, thus reducing the dimension of the matrix eigenvalue problem. Through a sequence of IT calculations for different thresholds and an a posteriori extrapolation of all observables to vanishing threshold, we can recover the full NCSM results up to extrapolation errors [15]. For $^{16,18}\text{C}$

the IT scheme allows us to extend our calculations to $N_{\max} = 8$ and to improve the reliability of our extrapolations.

II. RESULTS

A. Convergence and error estimates

For our detailed studies of observables we are looking for the region in which the N_{\max} -convergence is the fastest and the dependence on $\hbar\Omega$ is the smallest. This optimal frequency range can vary between different observables and different isotopes. We will use the N_{\max} -dependence of the binding energy and the first 2^+ excitation energy in the largest model spaces as our primary criterion for selecting the optimal frequency range. The largest model spaces that we were able to reach in the full-space NCSM calculations spanned from $N_{\max} = 10$ in ^{10}C , via $N_{\max} = 8$ in $^{12,14}\text{C}$, to $N_{\max} = 6$ in $^{16,18}\text{C}$ and $N_{\max} = 4$ in ^{20}C . The largest matrix dimension was $D = 1.4 \times 10^9$ for ^{18}C . However, using the IT-NCSM scheme we are able to obtain results also with $N_{\max} = 8$ for $^{16,18}\text{C}$. From plots such as Fig. 1, focusing in particular on the trend for large model spaces, we find that the $\hbar\Omega$ -range 10-14 MeV seems to work very well for these observables. This choice applies to the CDB2k-interaction for the whole range of carbon isotope.

Figure 2 shows several examples of the constrained-fit procedure for quadrupole moments and $B(\text{E}2)$ strengths. The results are plotted as a function of $1/N_{\max}$ for the selected range of HO frequencies. Infinite model space corresponds to $1/N_{\max} \rightarrow 0$. The grey error bands indicate the bounds obtained when fitting to N_{\max} -sequences for different $\hbar\Omega$ ranges. They form the basis for the uncertainty estimates. We note that the use of a range of frequencies usually include sequences that converge from above and from below. This allows a more precise determination of the extrapolated, final result. A particular exception to this behavior is the $B(\text{E}2)$ strength of ^{16}C , for which all sequences converge from below. This will be further commented below.

B. Binding energies and 2^+ state properties

In Figs. 3 and 4 we compare the calculated and experimental trends for binding energies, 2_1^+ excitation energies, and E2 observables for the carbon chain of isotopes. It is clear that

TABLE I: NCSM calculated E2 observables of $^{10-20}\text{C}$ compared with experimental results. NCSM results are obtained using the CDB2k interaction. The recommended values come from constrained extrapolations (see text for details).

	$E_{\text{exc}}(2_1^+) [\text{MeV}]$		$Q(2_1^+) [efm^2]$		$B(E2; 2_1^+ \rightarrow 0_1^+) [e^2fm^4]$	
	CDB2k	Exp	CDB2k	Exp	CDB2k	Exp
^{10}C	3.62(2)	3.354	-1.1 ± 1.2^a	—	10 ± 2^a	12.4(2.0)
^{12}C	3.49(3)	4.439	+6.19(20)	+6(3)	8.83(89)	7.94(66)
^{14}C	5.36(72)	7.012(4)	+4.71(23)	—	5.30(46)	3.74(50)
^{16}C	2.25(23)	1.766(10)	-3.21(19)	—	2.15(9)	$2.6(9)^a, 4.15(73)^a$
^{18}C	1.83(9)	1.620(20)	+3.82(4)	—	4.22(32)	$4.3(1.2)^a$
^{20}C	1.72(7)	1.588(22)	+4.20(32)	—	4.68(66)	$< 5.7^b, 7.5_{-1.8}^{+3.2c}$

^aStrong mixing of the first two 2^+ states. The estimate of ^{10}C E2 observables is obtained by studying the sums and ratios of results for both 2^+ states.

^aFrom Ref. [3]

^aFrom Ref. [2].

^bFrom Ref. [4]

^cFrom Ref. [5].

the CDB2k interaction underbinds these isotopes by 10-20 % while the INOY interaction provides additional binding. The positive two-neutron separation energy for ^{16}C is not reproduced, which is probably associated with a slower convergence of states with neutrons in the sd shell. Excitation energies are much easier to converge and we find a very good agreement with the experimental trend. The possible exception is the large 2_1^+ excitation energy of ^{14}C that is overpredicted with the INOY interaction.

Numerical results for 2_1^+ excitation energies and E2 observables are presented in Table I. We stress that no effective charges were used in our NCSM calculations and that there are no adjustable parameters. Our calculated $B(E2; 2_1^+ \rightarrow 0_1^+)$ agrees rather well with the most recent experimental data for the entire chain of isotopes. We note that the extrapolation of our ^{16}C $B(E2; 2_1^+ \rightarrow 0_1^+)$ results is challenging as, unlike for other carbon isotopes, the $B(E2)$ value increases with N_{max} in the whole investigated HO frequency range, see Fig 2. This makes the extrapolation procedure less accurate. Although our final result agrees well

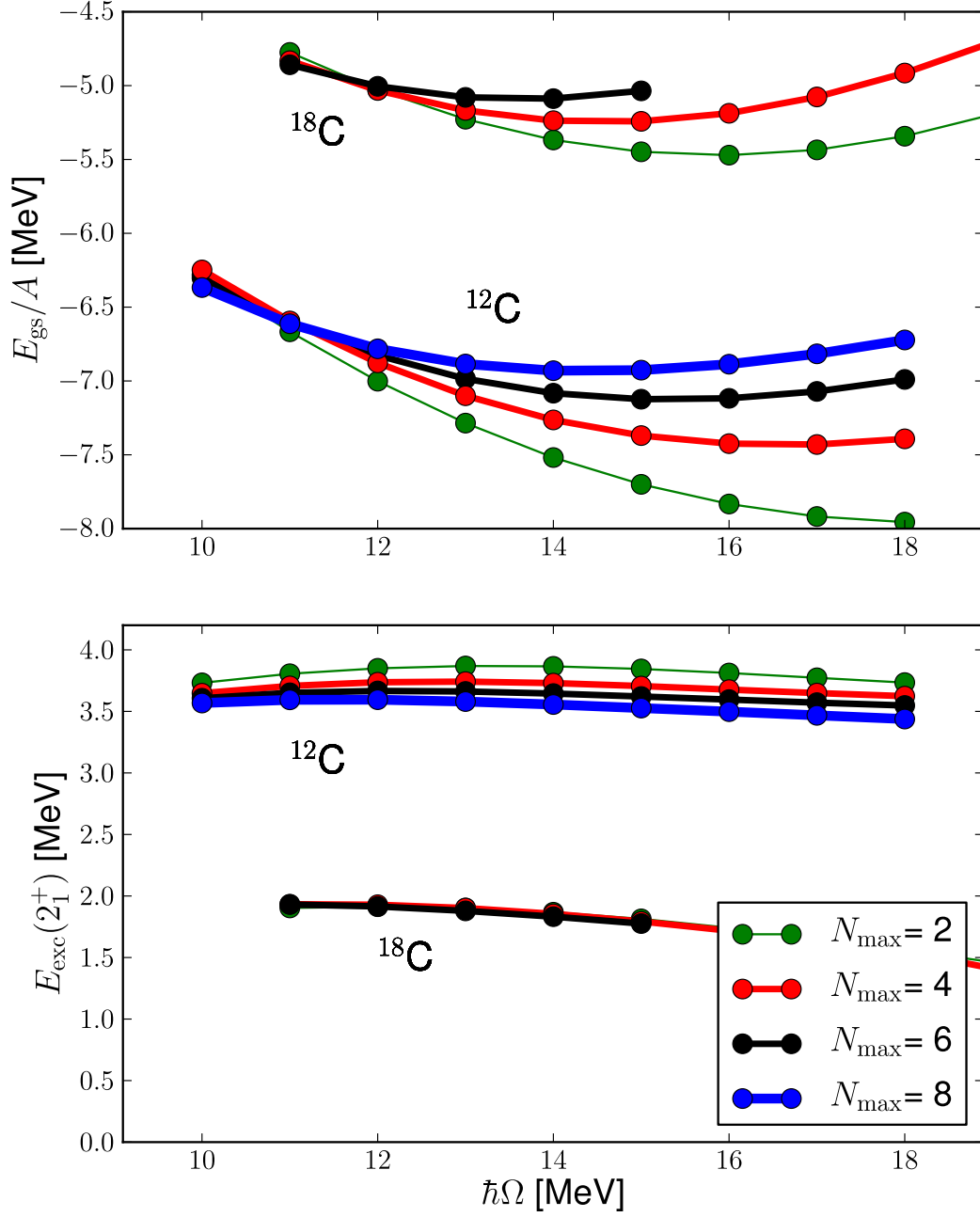


FIG. 1: (Color online) $\hbar\Omega$ -dependence for the ground-state energy (presented as E_{gs}/A) and the first 2^+ excitation energy for $^{12,18}\text{C}$. Each curve corresponds to a particular model space represented by the parameter N_{max} (see text for details).

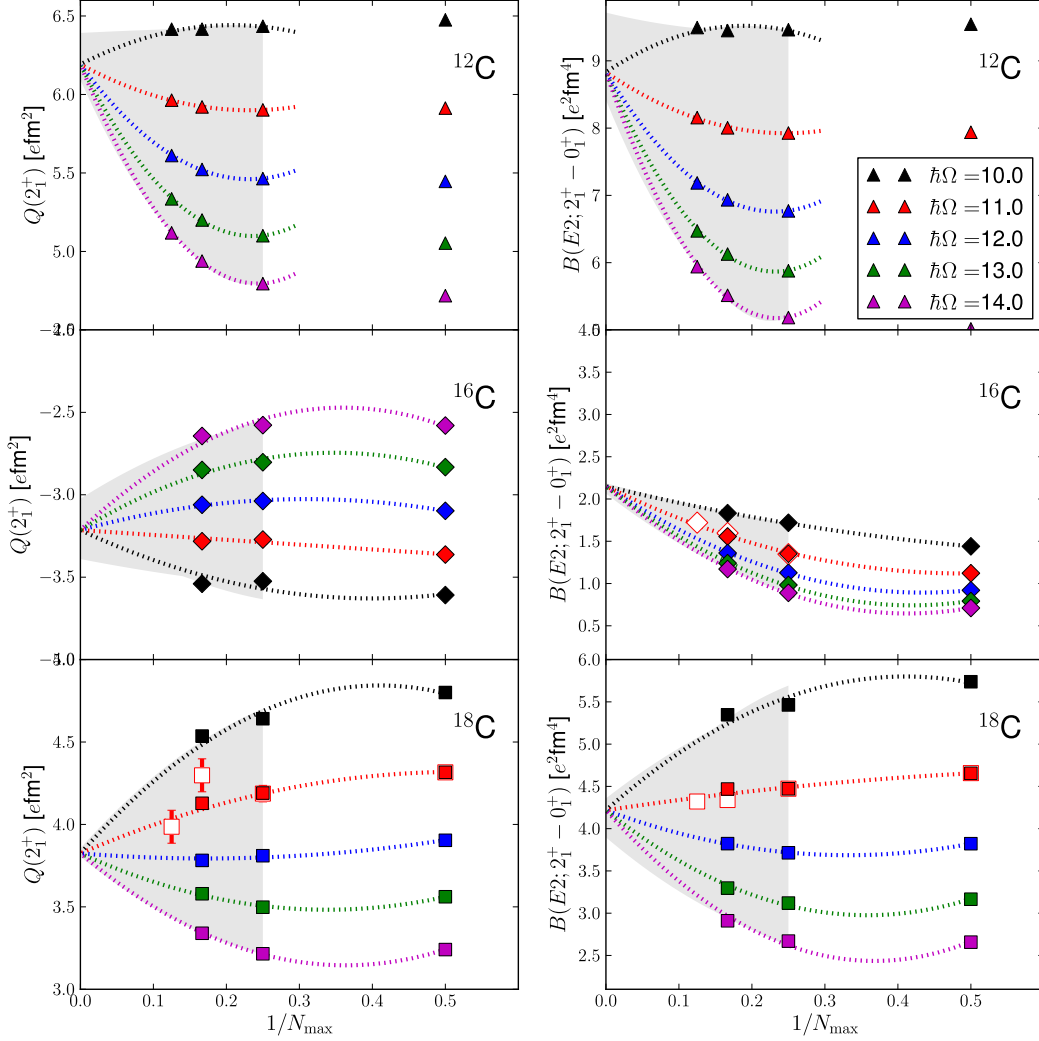


FIG. 2: (Color online) Model-space dependence of calculated E2 observables for $^{12,16,18}\text{C}$ in the NCSM. Results obtained with the CDB2k NN potential are presented as a function of $1/N_{\text{max}}$. Filled (open) symbols correspond to full (importance-truncated) space results. Dotted lines correspond to constrained fits to N_{max} -sequences at a fixed HO frequency. See also Table I.

with the data from RIKEN [3] it is slightly below the most recent experimental result from LBNL [2]. In addition, we note that our calculated quadrupole moment for the first 2^+ state of ^{16}C is $Q = -3.21 \pm 0.19 \text{ efm}^2$ while for $A = 12, 14, 18, 20$ we find the quadrupole moment of the 2_1^+ state to be positive.

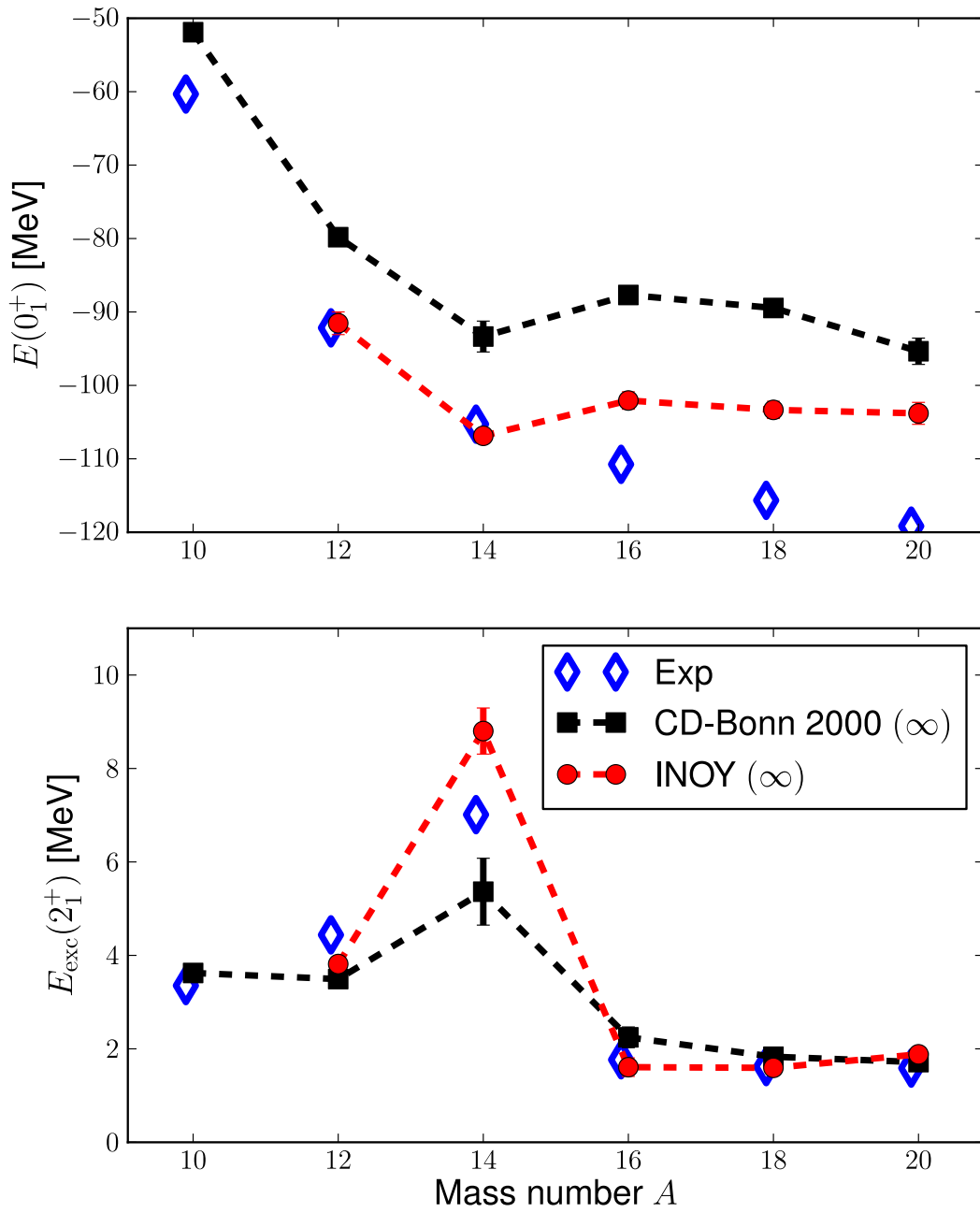


FIG. 3: (Color online) NCSM calculated binding energies and 2^+ excitation energies of $^{10-20}\text{C}$ compared with experimental results. Theoretical NCSM results are constrained extrapolations (see text for details).

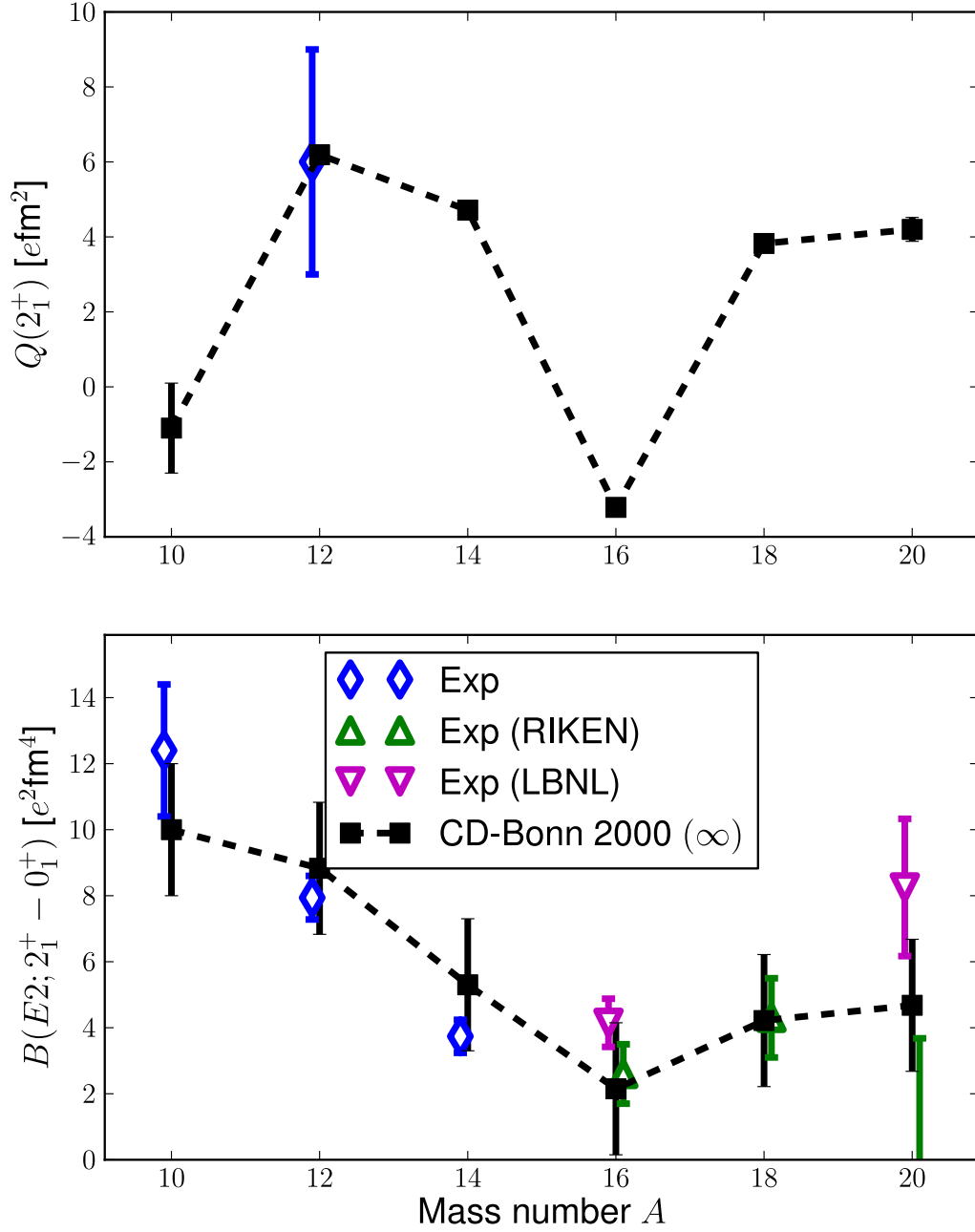


FIG. 4: (Color online) NCSM calculated E2 observables of $^{10-20}\text{C}$ compared with experimental results. See also Table I. NCSM results are obtained from constrained extrapolations (see text for details).

A qualitative understanding of these findings can be obtained by studying the mean occupation numbers of different single-particle states in the NCSM wave functions. In Fig. 5 these occupancies are plotted for the ground- and first 2^+ -state in the whole range of carbon isotopes. In particular for $^{14,16}\text{C}$ the excitation mechanisms are quite obvious. In ^{14}C the

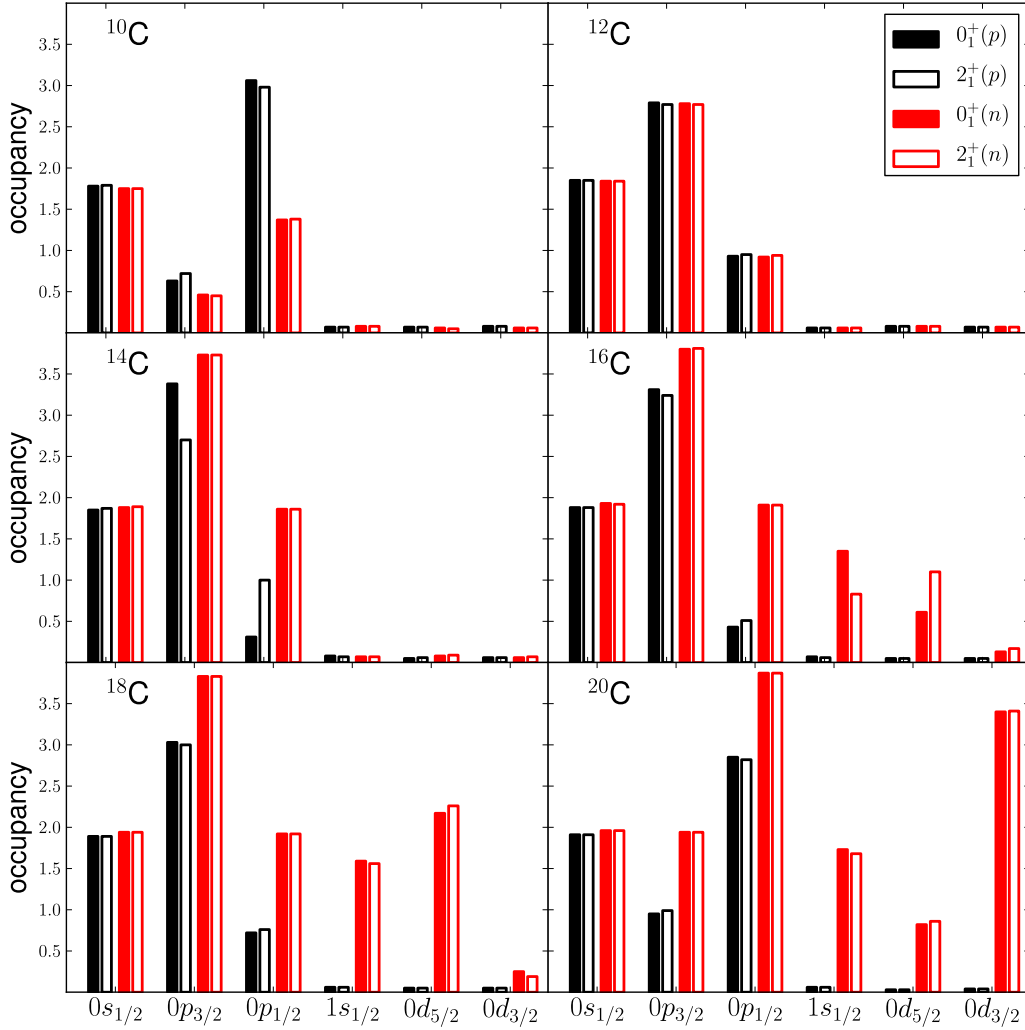


FIG. 5: (Color online) Occupation numbers for the ground- and first 2^+ -state in $^{10-20}\text{C}$ obtained with the CDB2k interaction. Black (red) bars on the left (right) correspond to proton (neutron) occupation numbers. Filled (open) bars correspond to the ground (2^+) state.

2_1^+ state corresponds to a proton excitation within the p shell, while in ^{16}C the 2_1^+ state is

TABLE II: Relative $B(E2)$ values for transitions among excited states of $^{14-20}\text{C}$. Results obtained with the CDB2k and INOY NN interactions are compared.

A	$\frac{B(E2; 2_2^+ \rightarrow 0_1^+)}{B(E2; 2_1^+ \rightarrow 0_1^+)}$		$\frac{B(E2; 2_2^+ \rightarrow 2_1^+)}{B(E2; 2_1^+ \rightarrow 0_1^+)}$	
	CDB2k	INOY	CDB2k	INOY
14	0.001	0.000	0.48	0.72
16	2.2	0.30	2.0	0.79
18	0.018	0.017	0.047	0.13
20	0.017	0.035	0.12	0.28

obtained through a re-configuration of neutrons in the sd shell. The value of the $B(E2)$ is quite sensitive to the fine details of the re-configuration and, as it involves the sd shell, we have a slower convergence in the NCSM.

For ^{10}C we observe a very strong mixing of the first two 2^+ states using the CDB2k interaction at small frequencies. To get at least crude estimates of the E2 properties of the 2_1^+ state we used a slightly different extrapolation approach: The ratios of, e.g., $Q(2_1^+)$ and $Q(2_2^+)$ was plotted for larger frequencies where the mixing is not observed, while the sum was plotted for the full range of frequencies. From such plots, for Q and $B(E2)$ observables, we can deduce estimates for $Q(2_1^+)$ and $B(E2; 2_1^+ \rightarrow 0_1^+)$ and their uncertainties. These are included in Table I and Fig. 4.

We note that the different NN interactions used in this study give very similar isotopic trends for E2 observables, but with a consistently smaller magnitude for the INOY interaction. This observation is connected to the anomalously large nuclear density generated by this interaction found already in ^4He calculations [23, 24].

Finally, a study of the characteristics of the second 2^+ state in these isotopes strengthens the conclusion of the prominence of ^{16}C in the structural evolution of the chain of even carbon isotopes. The sign of the quadrupole moment of this state, $Q(2_2^+)$, is reversed from $Q(2_1^+)$. I.e., it's negative for all isotopes except for ^{16}C . In addition, as summarized in Table II, the relative $B(E2)$ strength from this state to the ground state is much smaller than from the first 2^+ . These findings are obtained with both NN Hamiltonians used in this study. However, the relative transitions from the second 2^+ in ^{16}C stand out with a clear difference in the predictions of CDB2k and INOY, see Table II. As the INOY interaction

often hints to possible structural influence from NNN forces we continue our study in the next section with a more detailed investigation of the ^{16}C structure using chiral $NN+NNN$ Hamiltonians.

C. Higher-lying states of ^{16}C and the role of the NNN interaction

Transitions from higher excited states of ^{16}C were also studied in a recent experiment [25]. In particular, the transitions $2_2^+ \rightarrow 2_1^+$, $4_1^+ \rightarrow 2_1^+$ and $3_1^+ \rightarrow 2_1^+$ were observed. Interestingly, no transition from the 2_2^+ state to the ground state was seen. We performed additional calculations with different Hamiltonians to study higher excited states in ^{16}C and their electromagnetic transitions. In Fig. 6, we show the calculated and experimental energy levels of ^{16}C , and in Table III we summarize our calculated $B(E2)$ values among excited states normalized to $B(E2; 2_1^+ \rightarrow 0_1^+)$. In particular, we compare results obtained with SRG-transformed chiral NN and chiral $NN+NNN$ interactions, including the SRG-induced three-nucleon terms in both cases as discussed in Ref. [16], to those obtained with the CDB2k interaction. A striking feature is a strong suppression of the $2_2^+ \rightarrow 0_1^+$ transition when the initial NNN interaction is included. Clearly, the calculation without the NNN interaction contradicts the new MSU experiment [25]. From Table III we observe that relative E2 transition strengths obtained with the chiral NN interaction are similar to the ones obtained with the CDB2k interaction. Furthermore, we see from Table II that the relative $B(E2)$ calculated with the INOY interaction (that mimics some NNN effects) resemble results of the chiral $NN+NNN$ Hamiltonian. The sensitivity to the presence of the NNN interaction is remarkable. The $2_2^+ \rightarrow 0_1^+$ transition is suppressed by a factor of ~ 20 in the calculation with the NNN . The excitation energies of the lowest five ^{16}C excited states are also influenced by the NNN interaction as seen in Fig. 6. The agreement with experimental spectrum is quite reasonable in all presented cases, although slightly improved in the calculation with the chiral $NN+NNN$ Hamiltonian.

From Table III, we also note a strong sensitivity of the $3_1^+ \rightarrow 2_1^+$ transition to the presence of the NNN interaction. The calculation with the chiral $NN+NNN$ Hamiltonian predicts a strongly suppressed $B(E2; 3_1^+ \rightarrow 2_1^+)$ transition. This transition is observed, however [25]. Our calculation with the NNN interaction predicts this transition to be of M1 character as seen from Table IV. We also observe a sign change of the magnetic moments of both the 2_1^+

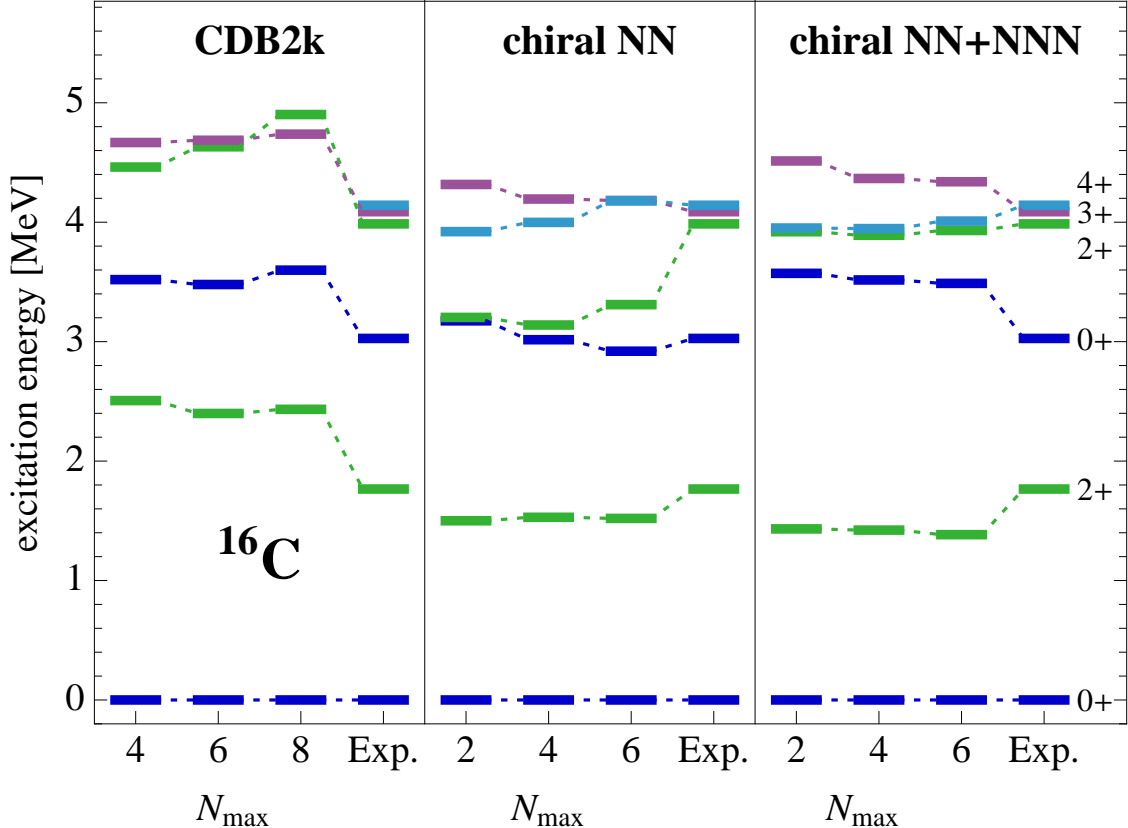


FIG. 6: (Color online) Excitation energies of the lowest states of ^{16}C . Calculations using the Lee-Suzuki-transformed CDB2k potential at $\hbar\Omega = 12$ MeV (left) and the SRG-evolved chiral NN and $NN+NNN$ interactions with $\Lambda = 1.88 \text{ fm}^{-1}$ for $\hbar\Omega = 16$ MeV (middle and right) are compared for different values of N_{max} to experiment.

and the 2_2^+ states in calculations with the NNN interaction included. The magnetic moment of the 3_1^+ state is unaffected, however. The sensitivity of the 2_1^+ magnetic moment to the NNN interaction we also find in ^{20}C (see Table IV).

Overall, we find a strong sensitivity of the electromagnetic observables in ^{16}C to the details of nuclear Hamiltonian. More detailed experimental study of higher excited states and their transitions would be quite useful.

III. CONCLUSION

In summary we have computed low-lying states of even carbon isotopes with $A = 10 - 20$ within the *ab initio* NCSM. We used several accurate nucleon-nucleon (NN) as well as NN

TABLE III: Relative $B(E2)$ values for transitions among excited states of ^{16}C . Results obtained with the CDB2k NN potential, the chiral NN , and the chiral $NN+NNN$ interaction are compared. For CDB2k the Lee-Suzuki effective interactions were used ($\hbar\Omega = 12$ MeV, $N_{\text{max}}=6$) and for the chiral interactions the SRG-evolved interactions ($\Lambda = 1.88 \text{ fm}^{-1}$, $\hbar\Omega = 16$ MeV, $N_{\text{max}}=6$) including the induced three-nucleon terms were used.

$\frac{B(E2; J_i \rightarrow J_f)}{B(E2; 2_1^+ \rightarrow 0_1^+)}$	CDB2k	chiral NN	chiral $NN+NNN$
$2_1^+ \rightarrow 0_1^+$	1	1	1
$2_2^+ \rightarrow 0_1^+$	2.2	0.75	0.11
$2_2^+ \rightarrow 2_1^+$	2.0	1.7	0.65
$3_1^+ \rightarrow 2_1^+$	0.36	0.31	0.02
$4_1^+ \rightarrow 2_1^+$	0.89	0.69	0.80

TABLE IV: Absolute values for magnetic dipole moments and $B(M1)$ transition strengths of excited states in $^{16,20}\text{C}$. Results obtained with the CDB2k NN potential and the chiral $NN+NNN$ interaction are compared. $B(M1)$ in μ_N^2 and μ in μ_N . Parameters as in Table III with $N_{\text{max}}=4$ for ^{20}C . The brackets indicate the uncertainties of the threshold extrapolation for the IT-NCSM.

	^{16}C		^{20}C	
	CDB2k	chiral $NN+NNN$	CDB2k	chiral $NN+NNN$
$B(M1; 2_2^+ \rightarrow 2_1^+)$	0.013	0.063	0.015	
$B(M1; 3_1^+ \rightarrow 2_1^+)$	0.17	0.17	0.013	
$\mu(2_1^+)$	0.13	-0.42	0.22	0.001(8)
$\mu(2_2^+)$	1.3	-0.79	0.58	
$\mu(3_1^+)$	-3.2	-3.1	0.016	

plus NNN interactions and calculated excitation energies of the lowest 2^+ state, the electromagnetic $B(E2; 2_1^+ \rightarrow 0_1^+)$ transition strengths, the 2_1^+ quadrupole moments and selected electromagnetic transitions among higher excited states. Unlike in the phenomenological shell model, our calculations do not include effective charges or any other fitting parameters.

Overall, we find a consistent NCSM description of the $B(E2; 2_1^+ \rightarrow 0_1^+)$ dependence on the mass number for the whole carbon isotopic chain from $A = 10$ to 20. However, our calculated $B(E2; 2_1^+ \rightarrow 0_1^+)$ values for ^{16}C , with different Hamiltonians, all underestimate the most recent experimental measurements. Also, we find a remarkable sensitivity of the transition rates from higher excited states in ^{16}C to the details of the nuclear interactions. The chiral $NN+NNN$ interaction gives the excitation spectrum of ^{16}C in a slightly better agreement with experiment than the CDB2k NN potential and, further, the former interaction predicts the suppression of the $2_2^+ \rightarrow 0_1^+$ transition in agreement with experimental observations. We find a strong sensitivity of the magnetic moments of the 2_1^+ state to the nuclear interaction in ^{16}C and ^{20}C and even more so for the 2_2^+ state in ^{16}C .

The NCSM calculations predict sign changes of the 2_1^+ quadrupole moments between different carbon isotopes. In particular, we predict a negative quadrupole moment in ^{16}C , a very small quadrupole moment in ^{10}C and a $B(E2; 2_1^+ \rightarrow 0_1^+)$ value in ^{10}C that is about the same as that in ^{10}Be . In ^{12}C , we obtain $Q(2_1^+) = +6.2(2) \text{ efm}^2$. It will be worth measuring these moments in the future.

Acknowledgments

We would like to thank A. Macchiavelli, P. Fallon, M. Wiedeking, and M. Petri for many useful discussions. Support from the European Research Council under the FP7, the NSERC grant No. 401945-2011, the Deutsche Forschungsgemeinschaft through contract SFB 634, the Helmholtz International Center for FAIR (HIC for FAIR), and the BMBF (06DA9040I) is acknowledged. Computing resources have been provided by the Jülich Supercomputing Centre and by LOEWE-CSC. Prepared in part by LLNL under Contract DE-AC52-07NA27344.

-
- [1] N. Imai, H. J. Ong, N. Aoi, H. Sakurai, K. Demichi, H. Kawasaki, H. Baba, Z. Dombrádi, Z. Elekes, N. Fukuda, et al., Phys. Rev. Lett. **92**, 62501 (2004).
 - [2] M. Wiedeking, P. Fallon, A. O. Macchiavelli, J. Gibelin, M. S. Basunia, R. M. Clark, M. Cromaz, M.-A. Deleplanque, S. Gros, H. B. Jeppesen, et al., Phys. Rev. Lett. **100**, 152501 (2008).

- [3] H. J. Ong, N. Imai, D. Suzuki, H. Iwasaki, H. Sakurai, T. K. Onishi, M. K. Suzuki, S. Ota, S. Takeuchi, T. Nakao, et al., *Phys. Rev. C* **78**, 14308 (2008).
- [4] Z. Elekes, Z. Dombrádi, T. Aiba, N. Aoi, H. Baba, D. Bemmerer, B. A. Brown, T. Furumoto, Z. Fülöp, N. Iwasa, et al., *Phys. Rev. C* **79**, 11302 (2009).
- [5] M. Petri, P. Fallon, A. O. Macchiavelli, S. Paschalis, K. Starosta, T. Baugher, D. Bazin, L. Cartegni, R. M. Clark, H. L. Crawford, et al., *Phys. Rev. Lett.* **107**, 102501 (2011).
- [6] S. Fujii, T. Mizusaki, T. Otsuka, T. Sebe, and A. Arima, *Physics Letters B* **650**, 9 (2007).
- [7] P. Navrátil, J. Vary, and B. R. Barrett, *Phys. Rev. Lett.* **84**(25), 5728 (2000).
- [8] P. Navrátil, S. Quaglioni, I. Stetcu, and B. R. Barrett, *J Phys G Nucl Partic* **36**(8), 083101 (2009).
- [9] R. Machleidt, *Phys. Rev. C* **63**, 24001 (2001).
- [10] P. Doleschall, *Phys. Rev. C* **69**, 54001 (2004).
- [11] D. R. Entem and R. Machleidt, *Phys. Rev. C* **68**, 41001 (2003).
- [12] D. Gazit, S. Quaglioni, and P. Navrátil, *Phys. Rev. Lett.* **103**, 102502 (2009).
- [13] E. Caurier and F. Nowacki, *Acta Physica Polonica B* **30**, 705 (1999).
- [14] E. Caurier, P. Navrátil, W. E. Ormand, and J. P. Vary, *Physical Review C (Nuclear Physics)* **64**, 51301 (2001).
- [15] R. Roth, *Phys. Rev. C* **79**, 64324 (2009).
- [16] R. Roth, J. Langhammer, A. Calci, S. Binder, and P. Navrátil, *Phys. Rev. Lett.* **107**(7), 072501 (2011).
- [17] P. Navrátil (2011), unpublished.
- [18] K. Suzuki and S. Lee, *Prog. Theor. Phys* **64**, 2091 (1980).
- [19] E. Jurgenson, P. Navratil, and R. Furnstahl, *Phys. Rev. Lett.* **103**(8), 82501 (2009).
- [20] C. Forssén, J. Vary, E. Caurier, and P. Navrátil, *Phys. Rev. C* **77**(2), 24301 (2008).
- [21] C. Forssén, E. Caurier, and P. Navrátil, *Phys. Rev. C* (2009).
- [22] R. Roth and P. Navrátil, *Phys. Rev. Lett.* **99**, 92501 (2007).
- [23] R. Lazauskas and J. Carbonell, *Phys. Rev. C* **70**, 44002 (2004).
- [24] E. Caurier and P. Navrátil, *Phys. Rev. C* **73**, 21302 (2006).
- [25] M. Petri (2011), private communication.